

148
NTIS HC \$3.25

X-661-72-432

PREPRINT

66114

X-RAY SOURCES IN THE GENERAL DIRECTION OF THE GALACTIC CENTER

P. J. SERLEMITOS
R. D. BLEACH
E. A. BOLDT
S. S. HOLT

NOVEMBER 1972

Reproduced by
NATIONAL TECHNICAL
INFORMATION SERVICE
U S Department of Commerce
Springfield VA 22151



— GODDARD SPACE FLIGHT CENTER —
GREENBELT, MARYLAND

1
(NASA-TM-X-66114) X-RAY SOURCES IN THE
GENERAL DIRECTION OF THE GALACTIC CENTER
P.J. Serlemitos, et al (NASA) Nov. 1972
21 p CSCL 03B

N73-12873

Unclas
49139
G3/29

20p.

X-RAY SOURCES IN THE GENERAL
DIRECTION OF THE GALACTIC CENTER

P. J. Serlemitsos, R. D. Bleach*, E.A. Boldt and S. S. Holt
Laboratory for High Energy Astrophysics
NASA/Goddard Space Flight Center
Greenbelt, Maryland 20771

ABSTRACT

We have measured spectra in the range 1.5 to 35 keV from six low galactic latitude sources near the direction of the galactic center and have found them to be generally consistent with thermal emission and, as a rule, to be depleted of low energy photons. An interpretation of the latter observation based on interstellar absorption places these sources toward the central region of the galaxy and sets their x-ray luminosity at $\geq 10^{38}$ ergs/sec for each. We have also observed the extended source 2U 1743-29 in near coincidence with the galactic center; our observation supports a power law spectrum and rejects a blackbody interpretation of the emission from this source.

*University of Maryland and Naval Research Laboratory

I. Introduction

X-Ray source position data from the early rocket surveys (Friedman, Byram and Chubb, 1967) and from the first x-ray satellite UHURU (Giacconi, et al, 1972) reveal two readily identifiable characteristics: 1. X-ray sources show an increased concentration near the plane of the galaxy; 2. there is additional clustering in galactic longitude within several degrees of the galactic center. Anisotropies in longitude were interpreted by Gursky, Gorenstein and Giacconi (1967) as indicating that x-ray sources are located in galactic spiral arms. Specifically, the group of sources in the general direction of the galactic center were placed in the Sagittarius arm, defined by optical data to be some 2 kpc away. Low energy spectra for these sources, however, have so far implied an amount of absorption which, if due to interstellar matter, gives distances considerably larger than 2 kpc (Gorenstein, Giacconi and Gursky, 1967; Rappaport, et al, 1969); such absorption would place the Sagittarius sources toward the central region of the galaxy.

It is always possible that any particular source may have a low energy cutoff caused by cold material near the source. We must assume, however, that x-ray sources are not generally imbedded in clumps of cold material because many other sources do not exhibit this large amount of absorption. At the same time, there is increasing indication that large absorption is generally characteristic of low galactic latitude sources (such as the Sagittarius sources discussed here), so that the hypothesis of low latitude sources generally being the most distant ones on the basis of their spatial distribution is supported by the observed spectra.

II. The Experiment

On 9 August 1971, we flew an experiment aboard an aerobee 170 rocket mainly for the purpose of studying possible galactic effects of the diffuse x-radiation (Bleach et al, 1972a). The detector complement consisted of two mutually aligned multi-anode gas proportional counters, identical in all respects, except that one had an argon-methane (P-10) gas mixture, while the other was filled with xenon and methane in similar proportions. The windows were in both cases 1-mil aluminized kapton. The collimation was 1.8×7.2 degrees FWHM. Total net effective area for each detector was 650 cm^2 . An ACS function required only for purposes of achieving the primary experiment goal brought the detector field of view near the center of the galaxy, with the 7.2 degree collimation direction lined up with the plane. A rapid scan in galactic longitude subsequently brought the low latitude sources in that region into the field of view.

In Table 1 we list all sources from the UHURU catalogue (Giacconi, et al, 1972) that should have contributed to the counting rate, at one time or another, during this scan. Also listed are galactic coordinates, maximum strengths, and variability measures for these sources. We make note of the fact that although we have listed the source 2U 1735-28, we have excluded it from further consideration since previous evidence indicates that this transient source should not have been detectable at the time of this observation (Kellogg, et al, 1971).

In Figure 1 we present the total count rate from both detectors as a function of time. Also shown at various points along the abscissa is the galactic longitude of the center of the detector field of view, as determined from aspect cameras. Note that from about +98 sec to +104 sec into the flight the payload was stationary and pointed at the position $l^{\text{II}} \approx 354^\circ$ $b^{\text{II}} \approx 0$. After the payload began to move the galactic latitude did not remain constant, but variations were slow and were confined to within .5 degrees of $b^{\text{II}} = 0$. We have superposed on the observed count rate a plot of a simulated rate based entirely on the source positions and strengths of Table 1. No effort was made to produce an absolute basis for comparison, but we have normalized the simulated rate to the observed one at the flat segment of these data, when the payload was pointed and the contributions of the various sources is better understood. Any differences between the two plots can be accounted for in terms of the variability measures of Table 1.

Due to the nature of this observation, the data suffer from considerable source confusion at all times. Nevertheless, we shall attempt to extract unique information from the observed spectra, at least in connection with the strongest of the sources on the list. What we hope to accomplish is 1) use the low-background data from the xenon-filled counter to extend the energy range of previous measurements, particularly with regard to making a choice between a thermal spectrum and a power law for some of the observed spectra; 2) take advantage of the redundancy afforded us by the two different counter gases to make a systematic-free evaluation of low energy absorption. Toward

accomplishing these goals, we have divided the exposure into five segments such that in each segment the bulk of the incident radiation comes from at most two known sources. To subtract the diffuse component we have selected data from a source free region centered at $\ell^{\text{II}} \simeq 60^\circ$ $b^{\text{II}} \simeq 0$; we recognize of course, the possibility of a small contamination of the net spectrum from a longitude dependent disk component. Spectral parameters for each segment pertain to the composite spectrum of these sources that contribute. Nevertheless, a number of conclusions can be drawn, some based in part on other existing spectral information. With regard to absorption, the amount of absorption we deduce for any one spectral group can only be a lower limit to the amount actually associated with a single contributing strong source. The last column in Table 1 shows the segment(s) to which each source mostly contributes.

III. Analysis

We will present the data in a representation that, we believe, best allows for comparisons with other observations. We have computed an incident spectrum $S(E)$ at energy E as follows:

$$S(E) = \frac{N_{\text{obs}}(E)}{\epsilon(E)} \quad (1)$$

where N_{obs} are the net observed counts from a source, and ϵ is an effective efficiency defined as

$$\epsilon(E) = \frac{N_{\text{calc}}(E)}{S'(E)} = \frac{C \int_0^\infty R(E, E') S'(E') dE'}{S'(E)} \quad (2)$$

$R(E, E')$ is the detector response function as determined from source calibrations, which relates the apparent energy to the incident true energy, $S'(E)$ is a first approximation to the source spectrum, and C is a normalization constant. A usual procedure for arriving at an approximate expression for $S(E)$ has been to use equation 2 for computing $N_{\text{calc}}(E)$, which is then compared with $N_{\text{obs}}(E)$ using the χ^2 method. This can be time consuming however, especially when $S(E)$ is best described using multiple parameters. In this paper we proceed to obtain better approximations for $S(E)$ using the above integral equation and starting with $S'(E) = \text{constant}$. For the counting statistics of these data and the spectra we have observed, this procedure converges rapidly, resulting in near final representation for $S(E)$ even after only one iteration. It is of course obvious that any sharp features of the incident spectrum, such as lines, will be smoothed over by an amount commensurate with the energy resolution of the instruments.

IV. Results

In Figure 2 we show the incident photon spectra that result from the last four segments of the exposure. Data from the two detectors are shown separately and with no normalization, other than what is intrinsic to the response functions. The solid line with each set of data depicts the analytical spectral shape that best fits both the argon and xenon points. In Table 2 we summarize the results of this analysis. n_H is the columnar hydrogen density to each source, implied by the amount of low energy absorption seen in the data, and computed

on the basis of Brown and Gould elemental abundances (Brown and Gould, 1970). We wish to point out the striking similarity of the four spectra, both with regard to the spectral shape and the values of the parameters. If we consider only the xenon points, we find that only in the case of spectrum 2 does a power law give almost as good a fit as a thermal continuum. In cases 4 and 5, a power law type spectrum was rejected with confidence exceeding 90%. The extended energy range made possible with xenon is essential in making this distinction. The statistical significance of the n_H values is such that the 90% confidence limits are less than a factor of two in all cases.

Source region 1 includes the important extended source 2U 1743-29 in near coincidence with the center of the galaxy. This source also contributes to the second segment but that contribution is masked by the more powerful neighboring sources. In segment 1, however, we have estimated that the two major sources contributing, i.e. 2U 1726-33 and the galactic center source, do so roughly in a 3:1 ratio in total counts. The incident spectrum inferred from the data of this segment is shown in Figure 3. It cannot be satisfactorily described in terms of a single exponential or a power law, as was the case with the other four spectra. The obvious guess would be that the two sources contributing have very different spectra. Characteristic of this spectrum is an apparent hardening above 15 keV, seen primarily in the xenon counter. At lower energies however, it is similar to the other four. A unique interpretation is possible if we

take into account a previous measurement of the galactic center source spectrum with data from the UHURU satellite (Kellogg, et al, 1971). This source apparently does have a hard spectrum in the UHURU energy range. Kellogg et al have given best fit parameters for the three most often used trial spectra, i.e. thermal, power law and blackbody with no obvious preference for any particular one. For comparison with our data, we have taken their spectra and combined them individually with a thermal spectrum that fits the data of this segment at lower energies. This introduces an additional parameter whose values however are constrained by the relative source strengths as given by UHURU and by the relative exposures obtained in this flight. We find that the best fit to the xenon data is obtained using the power law spectrum for 2U 1743-29. In Table 2 we list all relevant information concerning this fit. The thermal spectrum gave a worse but still acceptable fit. The blackbody spectrum, however, can be rejected with a high degree of confidence.

V. Conclusions

Our analysis supports a thermal model for the low latitude point sources in the general direction of the galactic center. Except for the large absorption at low energies, these sources appear spectrally similar to Sco X-1 and Cyg X-2. If the absorption is due to interstellar matter, they are at typical distances of 10 kpc, and therefore have intrinsic luminosities around 10^{38} ergs/sec. The temperatures and absorption measures that we have obtained are generally in agreement with those obtained by Gorenstein, Gursky and Giacconi (1967), Rappaport,

et al. (1969), and Tananbaum et al. (1971). One exception is the source GX 9+1 for which Rappaport et al find a lower absorption cutoff. Cruddace, et al. (1972), on the other hand, find much lower temperatures and generally lower cutoffs for three of the sources in Table 1 that they have observed. We do not understand the reason for these discrepancies but reiterate the generally excellent agreement between the independent argon and xenon data in this paper. Understandably, source confusion is a weak point of this analysis, but it would be difficult to miss an abundance of lower energy photons from any one of the stronger sources in the field of view.

Lewin, Ricker and McClintock (1971) have conducted a balloon survey of the general galactic center region and have detected hard x-rays, attributing them principally to a variable source which they named GX 1+4. This source was clearly out of our field of view. They also report the possible detection of hard x-rays from GX 3+1 and GX 5-1. This introduces the possibility of a variable hard component to the spectrum of these sources, as was shown to be the case with Sco X-1 (cf. Riegler, et al, 1970).

Lewin, Ricker and McClintock, have estimated an energy flux from GX 1+4 of $1.5 \text{ keV cm}^{-2} \text{ s}^{-1}$ in the range 18-50 keV. At $\sim 30 \text{ keV}$, where the galactic center source clearly dominates the composite spectrum of Figure 1, we estimate a differential flux of $.006 \text{ cm}^{-2} \text{ s}^{-1} \text{ keV}^{-1}$. This is in good agreement with the flux estimate at lower energies by Kellogg, et al. (1971). Based on the power law spectrum, our estimate of the flux in the energy range of Lewin et al is $.2 \text{ keV cm}^{-2} \text{ s}^{-1}$, or

well below that which they see from GX 1+4, and likely below their detection threshold.

Because of the nature of this observation our study has been restricted to the strong sources within 2 degrees of the disk and at small angles to the galactic center direction. This is a large sample of all low latitude luminous sources in the galaxy. From the UHURU catalogue we find some 12 such sources with strengths in excess of 100 count/sec, including the well known sources Cen X-3, Cyg X-3 and GX 340-0. Limited spectral information is available for most of the sources not already discussed in this paper. Focusing our attention to the low energy absorption, we list in Table 3 the relevant data for the entire group. Note that strong low energy absorption appears to be a general characteristic of these sources. This lends strong support to the interstellar nature of this absorption, although in some instances, (i.e. Cen X-3, GX 340-0) it has been proposed that the absorption is intrinsic to a model for the emission. If we accept the hypothesis that the absorption is primarily interstellar and that these sources have, therefore, large intrinsic luminosities, we conclude that the x-ray luminosity of the galaxy is primarily due to these few sources. This is not unlike the case of the Magellanic Clouds where Leong, et al. (1971), have found few luminous (10^{38} ergs/sec) sources making up almost the entire x-ray emission from these bodies.

These 12 sources form too small a group to allow us to undertake detailed considerations regarding their distribution in galactic

longitude. We note however that more than half of them are within 20 degrees of the galactic center. It is perhaps significant that galactic mass models (i.e. Innanen, 1966) show steep radial gradients. Observations also support highly anisotropic distributions in galactic longitude for most late-type stellar populations, so that we should expect to intercept correspondingly more of these objects in our line of sight at small angles to the galactic center than deduced from an assumed distribution consistent with early-type stars or the interstellar gas.

TABLE I.

UHURU Positions, Strengths, and Variability
Measures of Sources Relevant to This Observation, and
Segment(s) of the Exposure to Which Each Source Mostly Contributes

Source Designation							Spectral
UHURU	Other	ℓ^{II}	b^{II}	Strength (counts/sec)	Variability		Group
2U1718-39		348.81	-1.43	16 ± 2	-		1
2U1726-33	GX354-0	354.15	0.39	73	3		1
2U1735-28		359.57	1.56	565	≥ 10		-
2U1743-29	GCX	359.9	-0.3	40 ± 5	-		1,2
2U1744-26	GX3+1	2.28	0.83	460	3		2
2U1757-25	GX5-1	5.06	-0.99	1000	2		2,3
2U1758-20	GX9+1	9.07	1.17	600	2		3,4
2U1811-17	GX13+1	13.50	0.12	294 ± 4	-		4
2U1813-14	GX17+2	16.42	1.31	560	1.7		5

TABLE II.

Best Fit Spectrum for Each Group and Counter.
Also Given are the Corresponding χ^2 and Degrees of Freedom (f)

Spectral Group	Counter	Best Fit Spectrum	$n_H(\#/cm^2)$	χ^2	f
1	Ar	Th [*] (kT=4.9)	4.6×10^{22}	18.8	11
1	Xe	Th(kT=3.9)+PL ^{**} ($\alpha=.4$)	5.1×10^{22}	16.1	13
2	Ar	Th(kT=5)	2.9×10^{22}	10.5	10
2	Xe	Th(kT=5.6)	3.9×10^{22}	16.9	13
3	Ar	Th(kT=5.4)	2.5×10^{22}	8.7	9
3	Xe	Th(kT=5.8)	2.4×10^{22}	4.9	11
4	Ar	Th(kT=6.3)	3.6×10^{22}	10.6	9
4	Xe	Th(kT=5.4)	4.1×10^{22}	11.1	11
5	Ar	Th(kT=7.3)	2.7×10^{22}	9.3	10
5	Xe	Th(kT=6.4)	2.4×10^{22}	16.2	12

*Thermal $\frac{dN}{dE} \sim (e^{-\frac{E}{kT}})/E$

**Power Law $\frac{dN}{dE} \sim E^{-(1+\alpha)}$

TABLE III.

UHURU Sources Within 2 Degrees of the Disk and With Strengths in Excess of 100 Counts/sec. The Amount of Hydrogen to Each Source n_H is Inferred from Observed Cutoffs in the Spectra

Source Designation		$n_H(\#/cm^2) \times 10^{-22}$		
UHURU	Other	This Paper	Other	Reference
2U1735-28			3	1
2U1744-26	GX3+1	2.9-3.9	0.79, 0.58	2, 3
2U1757-25	GX5-1	2.4-3.9	2.2, 4.7	4, 5
2U1758-20	GX9+1	2.4-4.1	<.7, 3.3	4, 5
2U1811-17	GX13+1	3.6-4.1	4.2, 3.3	4, 5
2U1813-14	GX17+2	2.4-2.7	3.3, 2.5	5, 6
2U2030+40	CygX-3		4.7, 5.4	5, 7
2U1119-60	CenX-3		> 10	8
2U1516-56	Nor2		2.9, 0.79	3, 2
2U1630-47	GX337+0		7.1	2
2U1641-45	GX340-0		1.2	2
2U1704-42				

References

1. Kellogg, et al, 1971
2. Cruddace, et al, 1972
3. Hill, et al, 1972
4. Rappaport, et al, 1969
5. Gorenstein, Giacconi and Gursky, 1967
6. Tananbaum, et al, 1971
7. Bleach, et al, 1972b (revised value)
8. Giacconi, et al, 1971

REFERENCES

- Bleach, R. D., Boldt, E. A., Holt, S. S., Schwartz, D. A., and Serlemitsos, P. J. 1972, Ap. J. (Letters), 174, L101.
- Bleach, R. D., Boldt, E. A., Holt, S. S., Schwartz, D. A., and Serlemitsos, P. J. 1972, Ap. J. 171, 51.
- Brown, R. L. and Gould, R. J. 1970, Phys. Rev. D1, 2252.
- Cruddace, R., Bowyer, S., Lampton, M., Mack, J., and Margon, B. 1972, Ap. J. 174, 529.
- Friedman, H., Byram, E. T., and Chubb, T. A. 1967, Science 156, 374.
- Giacconi, R., Murray, S., Gursky, H., Kellogg, E., Schreier, E., and Tananbaum, H. 1972,
- Giacconi, R., Gursky, H., Kellogg, E., Schreier, E., and Tananbaum, H. 1971, Ap. J. (Letters) 167, L67.
- Gorenstein, P., Giacconi, R., and Gursky, H. 1967, Ap. J. (Letters) 150, L85.
- Gursky, H., Gorenstein, P., and Giacconi, R. 1967, Ap. J. (Letters) 150, L75.
- Hill, R. W., Burginyon, G., Grader, R. J., Palmieri, T.M., Seward, F. D., and Stoering, J. P. 1972, Ap. J. 171, 519.
- Innanen, K. A. 1966, Ap. J. 143, 153.
- Kellogg, E., Gursky, H., Murray, S., Tananbaum, H., and Giacconi, R. 1971, Ap. J. (Letters) 169, L99.
- Leong, C., Kellogg, E., Gursky, H., Tananbaum, H., and Giacconi, R., 1971, Ap. J. (Letters) 170, L67.

Lewin, W. H. G., Ricker, G. R., and McClintock, J. E., 1971,

Ap. J. (Letters) 169, L17.

Rappaport, S., Bradt, H. V , Navanan, S., and Spada, G. 1969,

Nature 221, 428.

Riegler, G. R., Boldt, E., and Serlemitsos, P. 1970, Nature 226, 1041.

Tananbaum, H., Gursky, H., Kellogg, E., and Giacconi, R. 1971,

Ap. J. (Letters) 168, L25.

FIGURE CAPTIONS

Figure 1 - Total count rate from both detectors as a function of time along with a simulated rate based on UHURU source positions and strengths. Shown at points along the abscissa is the galactic longitude of the center of the detector field of view.

Figure 2 - Inferred incident spectra for segments 2, 3, 4, and 5 of the exposure. Data points from the argon and xenon counters are shown separately. Solid lines depict the simple analytical spectral shapes that best fit the data in each spectrum.

Figure 3 - Inferred incident spectrum for segment 1 of the exposure. An acceptable fit requires a complex trial spectrum to accomodate an apparent hardening above 15 keV.

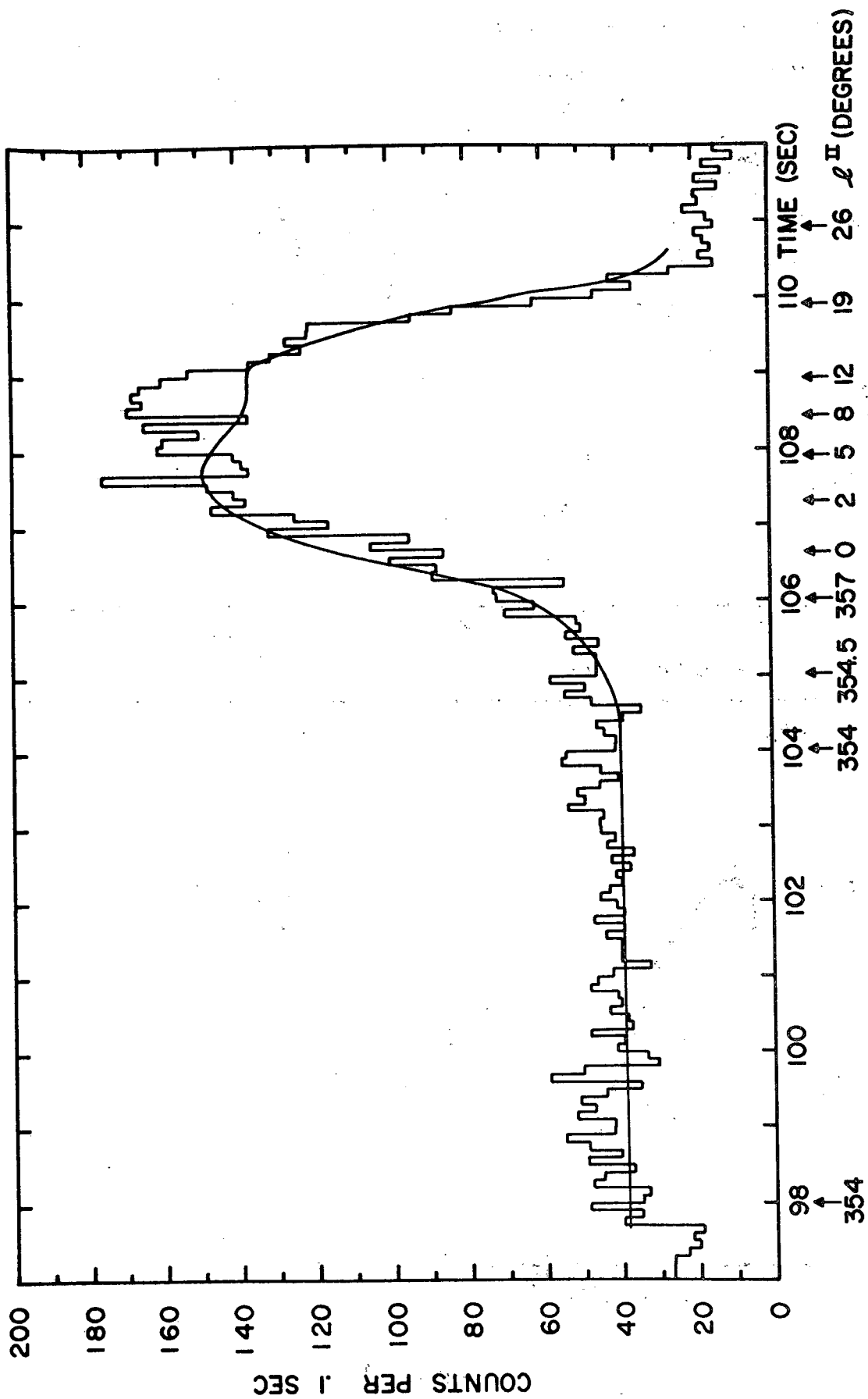


Fig. 1

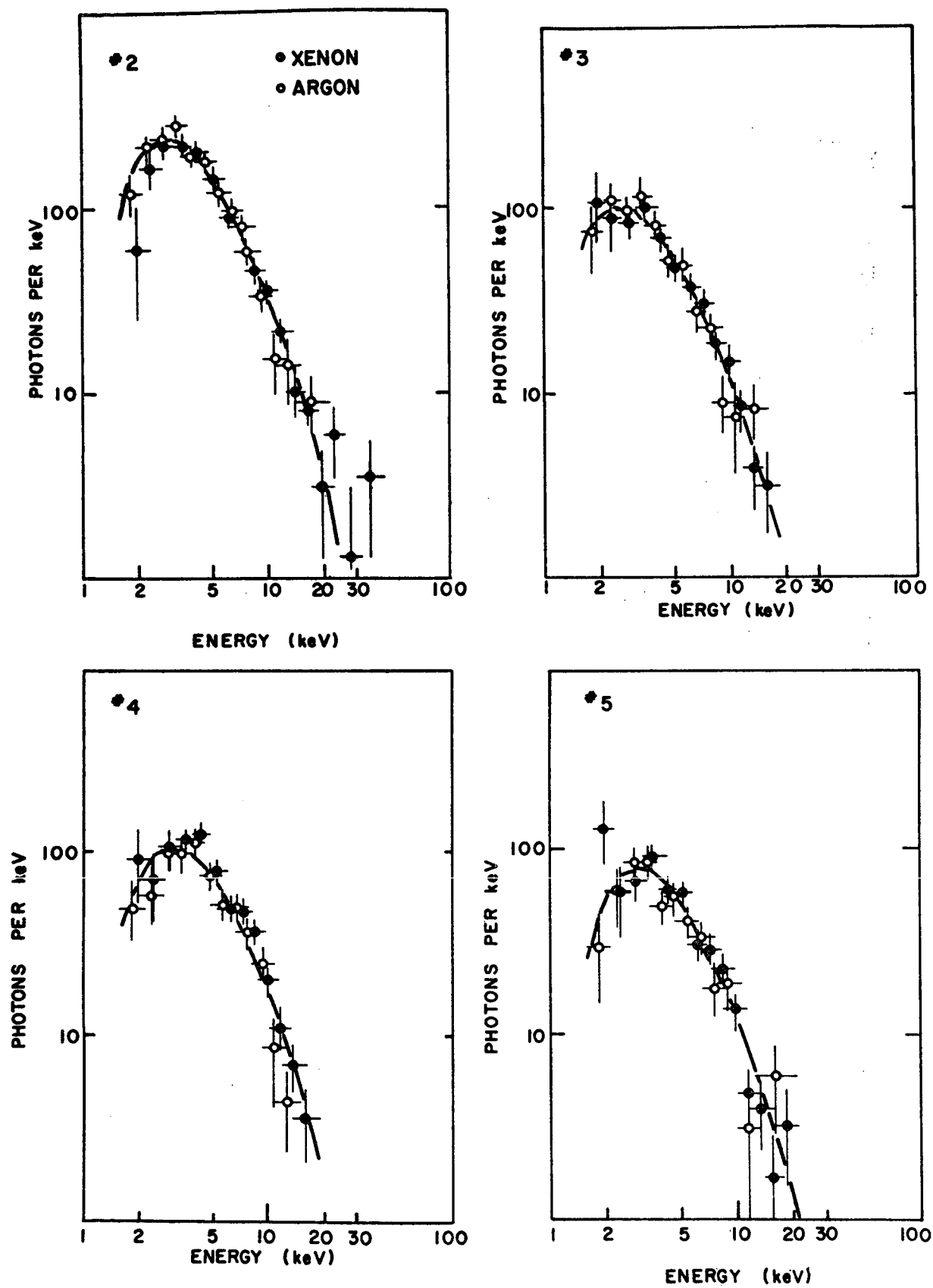


Fig. 2

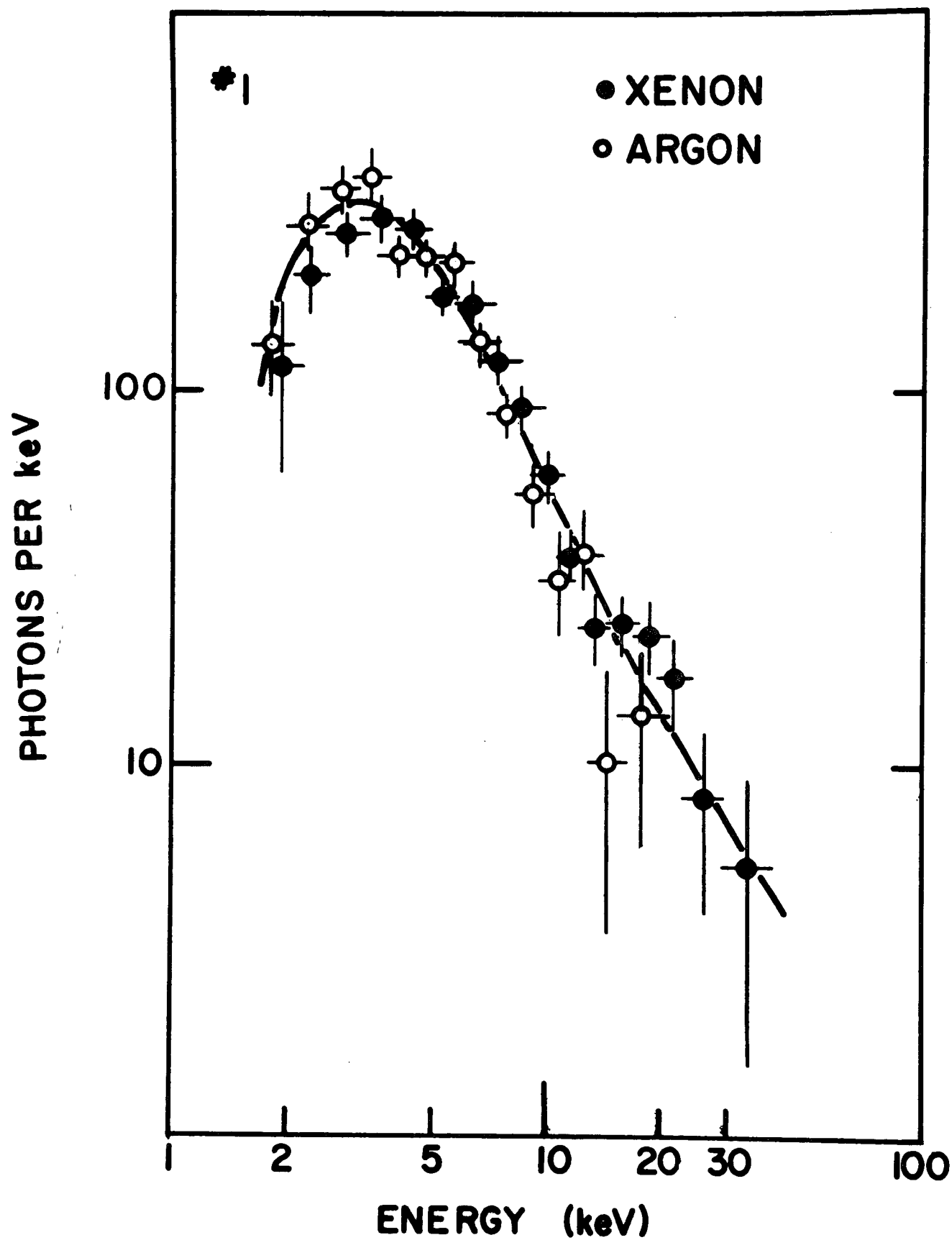


Fig. 3